

# Non-degenerate Priors for Arbitrarily Deep Networks

Anonymous Author(s)

Affiliation

Address

email

## Abstract

A good latent representation captures all the relevant degrees of freedom of the manifold on which the data live. We show, for typical deep architectures, that as the number of layers increase, the representational capacity of the model tends to capture fewer degrees of freedom. In the limit, deep representations only retain a single degree of freedom locally. In addition, gradient-based learning becomes intractable. We propose several solutions to address these pathologies.

## 1 Introduction

Deep networks have become an important tool for machine learning [cite]. However, training these models are difficult. Many arguments have been made for the need for deep architectures [cite Bengio]. However, it is hard to know what effect the deepness of an architecture has. Also, the weights don't necessarily move that much from their initialization.

### 1.1 Desirable properties of latent representations

Rifai et al. [2011a] make the point that a good latent representation is one that remains invariant when moving in directions orthogonal to the manifold that the data lie on. Conversely, a good latent representation must also change in directions tangential to the data manifold - otherwise we are losing information about the data.

## 2 The Jacobian of Deep GPs

**Deep Gaussian Processes** We introduce a generative non-parametric model to address this problem. Our approach is based on the GP-LVM [Lawrence [2004], Salzmman et al. [2008], Lawrence and Urtasun [2009], a flexible nonparametric density model. Deep Gaussian processes [Damianou and Lawrence [2012].

**The derivatives of a function drawn from a GP prior with a product kernel are i.i.d. Normal**

Because differentiation is a linear operator, the derivatives of a function drawn from a GP prior are also jointly Gaussian distributed, with covariance between derivatives w.r.t. different dimensions of  $\mathbf{x}$  given by:

$$\text{cov} \left( \frac{\partial f(\mathbf{x})}{\partial x_{d_1}}, \frac{\partial f(\mathbf{x})}{\partial x_{d_2}} \right) = \frac{\partial^2 k(\mathbf{x}, \mathbf{x}')}{\partial x_{d_1} \partial x'_{d_2}} \Big|_{\mathbf{x}=\mathbf{x}'} \quad (1)$$

[Solak et al. [2003]

If our kernel is a product over individual dimensions  $k(\mathbf{x}, \mathbf{x}') = \prod_d k_d(x_d, x'_d)$ , as in the case of the isotropic squared-exp kernel, then the diagonal covariances are given by  $\frac{\sigma_o^2}{\ell^2}$ , and the off-diagonal entries are zero. This means that elements are independent and identically distributed.

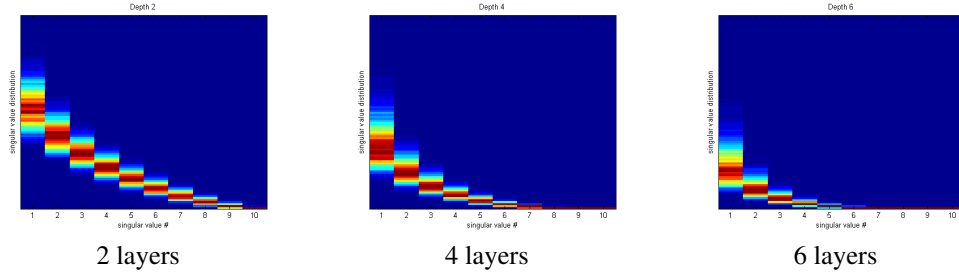


Figure 1: Singular value spectrum of the Jacobian of a deep GP. As the net gets deeper, the largest singular value dominates. This implies that there is only one effective degree of freedom in representation being computed.

**The elements of the Jacobian of a GP with an isotropic SE kernel are i.i.d. Gaussians** The Jacobian of the  $\ell^{\text{th}}$  function is:

$$J_{\mathbf{x} \rightarrow \mathbf{y}}^{\ell}(\mathbf{x}) = \begin{bmatrix} \frac{\partial f_1^{\ell}(\mathbf{x})}{\partial x_1} & \cdots & \frac{\partial f_1^{\ell}(\mathbf{x})}{\partial x_D} \\ \vdots & \ddots & \vdots \\ \frac{\partial f_D^{\ell}(\mathbf{x})}{\partial x_1} & \cdots & \frac{\partial f_D^{\ell}(\mathbf{x})}{\partial x_D} \end{bmatrix} \quad (2)$$

Because we’ve assumed that the GP on each output dimension  $f_d(\mathbf{x}) \sim \mathcal{GP}$  is independent, it follows that for a given  $\mathbf{x}$ , each row of  $J_{\mathbf{x} \rightarrow \mathbf{y}}^{\ell}(\mathbf{x})$  is independent. Above, we showed that the elements of each row are independent. This means that each entry in the Jacobian of a GP-distributed transformation is i.i.d. Normal.

**The Jacobian of a deep GP is a product of random normal matrices** By the multivariate chain rule, the derivative (Jacobian) of any compositions of functions is simply the product of the Jacobians of each function. and the Jacobian of the composed (deep) function is:

$$J^{1:L}(x) = \prod_{\ell=1}^L J^{\ell}(x) \quad (3)$$

Combining these results, we can analyze the representational properties of a deep Gaussian process by simply examining the properties of products of i.i.d. Gaussian matrices.

We follow [Rifai et al. \[2011b\]](#) in characterizing the representational properties of a function by the singular value spectrum of the Jacobian. Figure 1 shows the spectrum for deep GPs of different depths.

## 2.1 Fixing the filamentation pathology

**Attempted definition of a filament** A continuous, twice-differentiable region of a pdf is called a *filament* to the degree that, weighted by density, only one eigenvalue of the Hessian of the pdf are is small relative to the average eigenvalue.

Follow a suggestion in [Neal \[1995\]](#), we can fix the pathologies exhibited in figures 2 and 3 by simply making each layer of computation depend not only on the output of the previous layer, but also on the original input  $\mathbf{x}$ . Draws from the resulting priors are shown in figures 4 and 5.

## 3 Arbitrarily Deep Kernels

These types of kernels were originally investigated by [Cho \[2012\]](#). In this section, we take the infinite limits of these compositions, and propose a new variant.

One can derive a Gaussian process as a neural network:  $f(x) = \alpha^T \Phi(x) = \sum_{i=1}^K \alpha_i \phi_i(x)$ . We can consider applying the feature transform  $\Phi(\cdot)$  to the features themselves:  $\Phi_2 = \Phi(\Phi(\mathbf{x}))$ ,

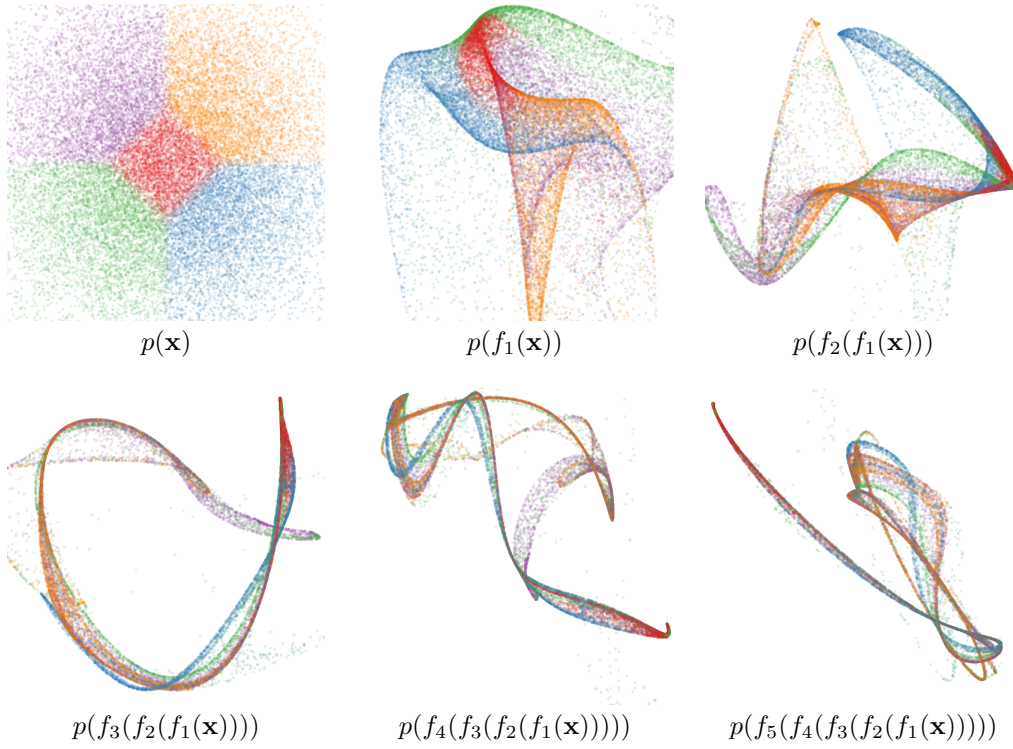


Figure 2: Draws from a deep GP. A distribution is warped by successive functions drawn from a GP prior. As the number of layers increases, the density exhibits a sort of filamentation.

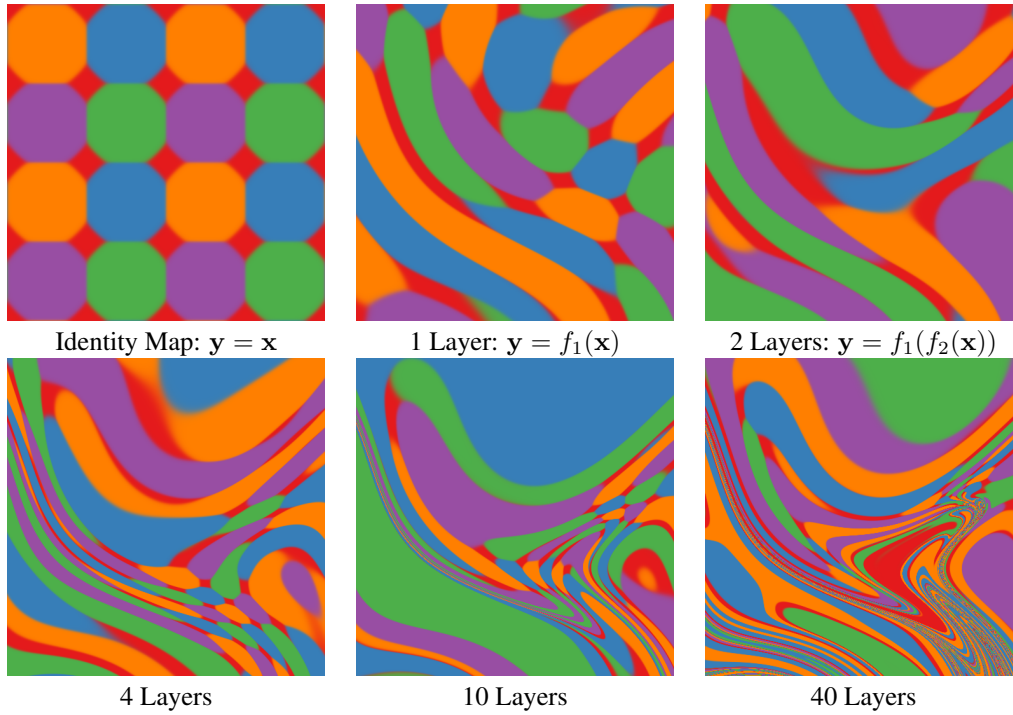


Figure 3: Feature Mapping of a deep GP. Shown here are the colors corresponding to the location  $\mathbf{y} = f(\mathbf{x})$  that each point is mapped to after being warped by a deep GP. This figure can be seen as the inverse of figure 2. Just as the densities in 2 became locally one-dimensional, there is locally only one direction that one can move  $\mathbf{x}$  in to change  $\mathbf{y}$ .

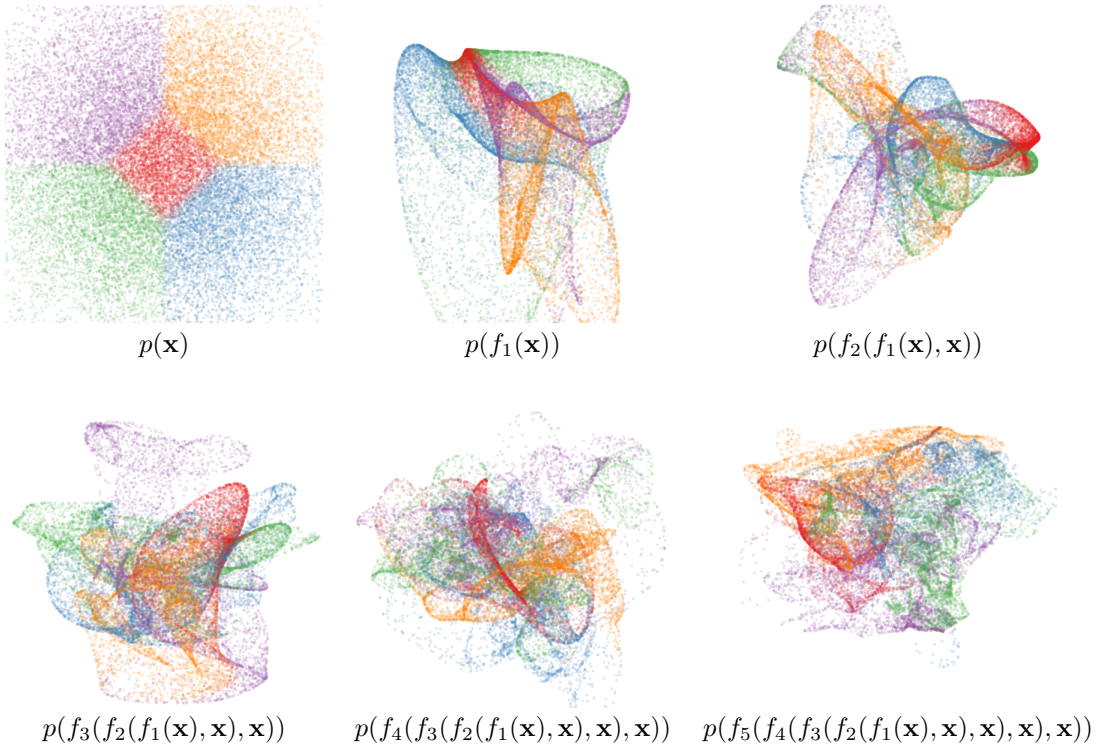


Figure 4: Draws from a deep GP, with each layer connected to the input  $\mathbf{x}$ . By always depending on the original input, the density becomes more complex without concentrating along filaments.

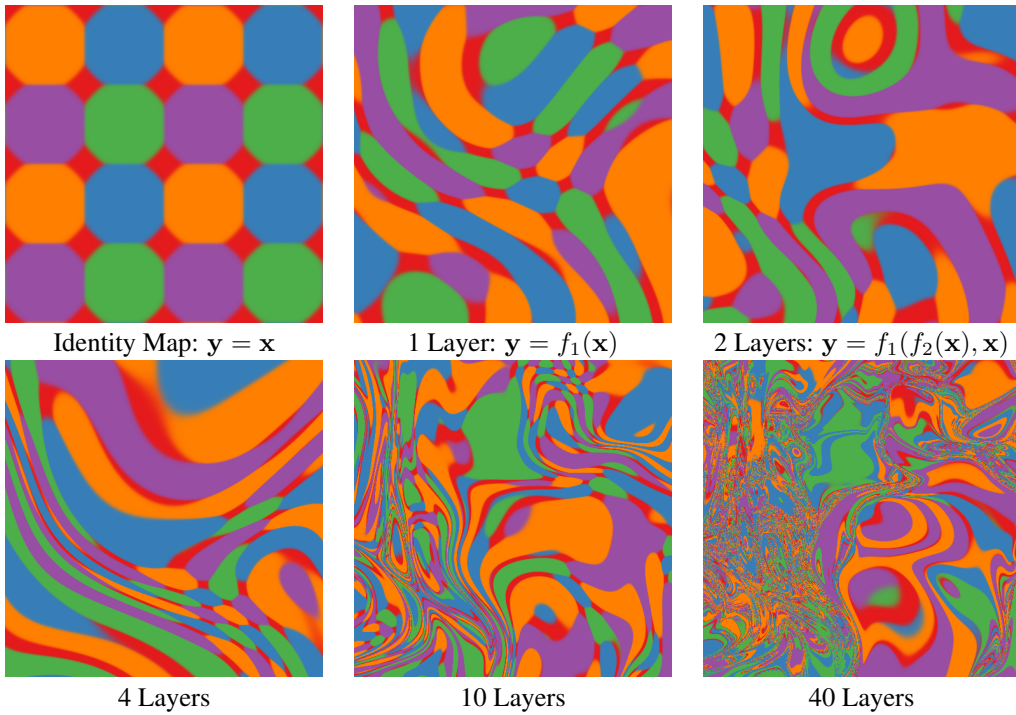
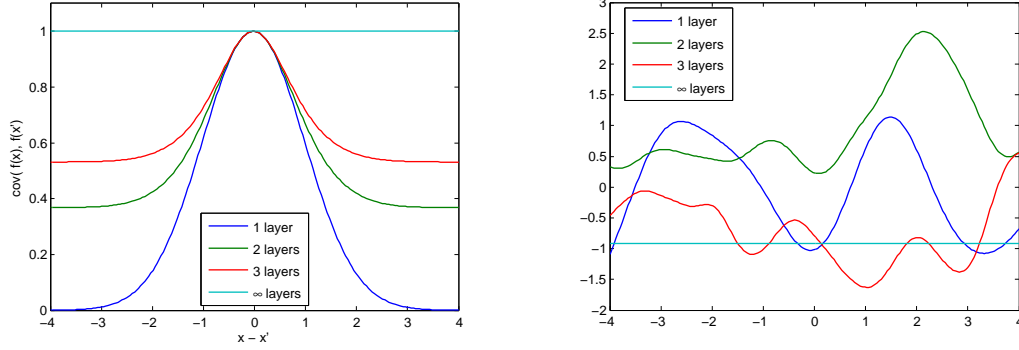


Figure 5: Feature Mapping of a deep GP with each layer connected to the input  $\mathbf{x}$ . Just as the densities in 4 become remain locally two-dimensional even after many transformations, in this mapping there are locally usually two directions that one can move  $\mathbf{x}$  in to change  $\mathbf{y}$ .



Kernel derived from iterated feature transforms

Draws from the corresponding kernel

Figure 6: A degenerate kernel produced by repeatedly applying a feature transform.

In this section, we derive a kernel which corresponds to arbitrarily many compositions of the feature vectors corresponding to the squared-exp kernel:

$$k_2(\mathbf{x}, \mathbf{x}') = \exp \left( -\frac{1}{2} \|\Phi(\mathbf{x}) - \Phi(\mathbf{x}')\|_2^2 \right) \quad (4)$$

$$k_2(\mathbf{x}, \mathbf{x}') = \exp \left( -\frac{1}{2} \sum_i [\phi_i(\mathbf{x}) - \phi_i(\mathbf{x}')]^2 \right) \quad (5)$$

$$k_2(\mathbf{x}, \mathbf{x}') = \exp \left( -\frac{1}{2} \sum_i [\phi_i(\mathbf{x})^2 - 2\phi_i(\mathbf{x})\phi_i(\mathbf{x}') + \phi_i(\mathbf{x}')^2] \right) \quad (6)$$

$$k_2(\mathbf{x}, \mathbf{x}') = \exp \left( -\frac{1}{2} \left[ \sum_i \phi_i(\mathbf{x})^2 - 2 \sum_i \phi_i(\mathbf{x})\phi_i(\mathbf{x}') + \sum_i \phi_i(\mathbf{x}')^2 \right] \right) \quad (7)$$

$$k_2(\mathbf{x}, \mathbf{x}') = \exp \left( -\frac{1}{2} [k_1(\mathbf{x}, \mathbf{x}) - 2k_1(\mathbf{x}, \mathbf{x}') + k_1(\mathbf{x}', \mathbf{x}')] \right) \quad (8)$$

$$k_2(\mathbf{x}, \mathbf{x}') = \exp(k_1(\mathbf{x}, \mathbf{x}') - 1) \quad (9)$$

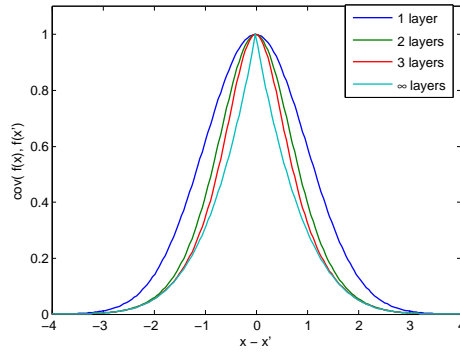
Thus if  $k_1(x, y) = e^{-\|x-y\|^2}$ , then the two-layer kernel is simply  $k_2(x, y) = e^{k_1(x, y)-1}$ . This formula is true for every layer:  $k_{n+1}(x, y) = e^{k_n(x, y)-1}$ . Note that nothing in this derivation depends on details of  $k_1$ , except that  $k_1(\mathbf{x}, \mathbf{x}) = 1$ . Because this is true for  $k_2$  as well, this recursion holds in general, and we have that  $k_{n+1}(x, y) = e^{k_n(x, y)-1}$ . In the infinite limit, this recursion converges to  $k(x, y) = 1$  for all inputs.

Figure 6 shows this kernel at different depths, including the degenerate limit. One interpretation of why repeated feature transforms lead to this degenerate prior is that each layer can only lose information about the previous set of features. In the limit, the transformed features contain no information about the original input  $\mathbf{x}$ . Since the function doesn't depend on its input, it must be the same everywhere.

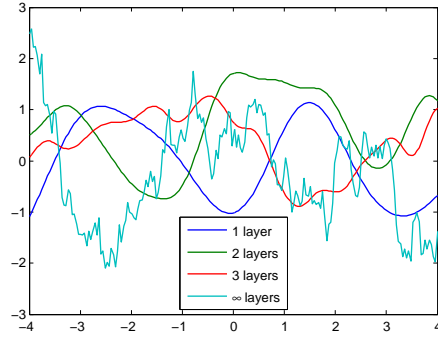
### 3.1 Fixing the deep kernel

Follow a suggestion from Radford Neal's thesis [Neal \[1995\]](#), we connect the inputs to each layer of features. We do this simply by augmenting the feature vector  $\Phi_n(\mathbf{x})$  with the extra features  $\mathbf{x}$  at





Kernel derived from iterated feature transforms  
with all layers connected to the input



Draws from the corresponding kernel

Figure 7: A non-degenerate version of the infinitely deep feature transform kernel. By connecting the inputs  $\mathbf{x}$  to each layer, the function can still depend on its input even after arbitrarily many layers of computation.

every layer:

$$k_{n+1}(\mathbf{x}, \mathbf{x}') = \exp \left( -\frac{1}{2} \left\| \begin{bmatrix} \Phi_n(\mathbf{x}) \\ \mathbf{x} \end{bmatrix} - \begin{bmatrix} \Phi_n(\mathbf{x}') \\ \mathbf{x}' \end{bmatrix} \right\|_2^2 \right) \quad (10)$$

$$k_{n+1}(\mathbf{x}, \mathbf{x}') = \exp \left( -\frac{1}{2} \sum_i [\phi_i(\mathbf{x}) - \phi_i(\mathbf{x}')]^2 - \frac{1}{2} \|\mathbf{x} - \mathbf{x}'\|_2^2 \right) \quad (11)$$

$$k_{n+1}(\mathbf{x}, \mathbf{x}') = \exp \left( k_1(\mathbf{x}, \mathbf{x}') - 1 - \frac{1}{2} \|\mathbf{x} - \mathbf{x}'\|_2^2 \right) \quad (12)$$

Thus, this kernel satisfies the recurrence  $k - \log(k) = 1 + \frac{1}{2} \|\mathbf{x} - \mathbf{x}'\|_2^2$ .

**Properties of this kernel** The solution to this recurrence has no closed form, but it is continuous and differentiable everywhere except at  $\mathbf{x} = \mathbf{x}'$ .

Conjectures:

- Samples from a GP with this prior are not differentiable.
- This kernel has smaller covariance than the squared-exp everywhere except at  $\mathbf{x} = \mathbf{x}'$ .
- Samples from this kernel are fractal.

## 4 Related Work

### 4.1 A Survey of deep architectures

#### Deep Density Networks

**Bayesian Deep Networks** Adams et al. [2010] developed a prior on finite but unboundedly deep neural networks, each layer having a finite but unbounded number of hidden units.

**Sum-product networks** introduced by Poon and Domingos [2011].

**Feature Composition Kernels** Cho [2012] developed kernels of the type discussed in section 4, and investigated them experimentally.

#### Recurrent Neural Networks

**Dynamical Systems** These architectures are all constructed in a stacked manner, with connections only between adjacent layers.

[Warping a 1d uniform distribution]

## 4.2 Related Analyses

Montavon et al. [2010] note that performance of a MLP degrades as the number of layers with random weights increases.

## 5 Conclusions

**Deep neural networks and deep Gaussian processes are analyzable using random matrix theory.** After proving that the Jacobian is an i.i.d. Gaussian matrix, many other forms of

**If you want to use very deep nets, you won't be able to do so if you initialize/regularize all your weights independently** We might want to think about different ways of

**If you initialize independently, the density becomes fractal** Points close in  $x$ -space can be very far in  $y$ -space, and vice versa.

**A spikey eigenspectrum will lead to saturation** Maybe we should initialize differently in order to avoid such saturation, like Martens' sparse initialization: [http://www.cs.toronto.edu/~jmartens/docs/Deep\\_HessianFree.pdf](http://www.cs.toronto.edu/~jmartens/docs/Deep_HessianFree.pdf)

## Acknowledgments

We would like to thank Andrew McHutchon, Neil Lawrence, Josh Tenenbaum, Andreas Diamanidou, James Lloyd, and Mark van der Wilk for helpful discussions.

## References

- Ryan P Adams, Hanna M Wallach, and Zoubin Ghahramani. Learning the structure of deep sparse graphical models. In *International Conference on Artificial Intelligence and Statistics*, pages 1–8, 2010.
- Youngmin Cho. *Kernel methods for deep learning*. PhD thesis, University of California, San Diego, 2012.
- Andreas C Damianou and Neil D Lawrence. Deep gaussian processes. *arXiv preprint arXiv:1211.0358*, 2012.
- N.D. Lawrence. Gaussian process latent variable models for visualisation of high dimensional data. *Advances in Neural Information Processing Systems*, 16:329–336, 2004.
- N.D. Lawrence and R. Urtasun. Non-linear matrix factorization with Gaussian processes. In *Proceedings of the 26th Annual International Conference on Machine Learning*, pages 601–608. ACM, 2009.
- Grégoire Montavon, Dr Braun, Klaus-Robert Müller, et al. Layer-wise analysis of deep networks with gaussian kernels. *Advances in Neural Information Processing Systems (NIPS)*, 23:1678–1686, 2010.
- Radford M Neal. *Bayesian learning for neural networks*. PhD thesis, University of Toronto, 1995.
- Hoifung Poon and Pedro Domingos. Sum-product networks: A new deep architecture. In *Computer Vision Workshops (ICCV Workshops), 2011 IEEE International Conference on*, pages 689–690. IEEE, 2011.
- Salah Rifai, Grégoire Mesnil, Pascal Vincent, Xavier Muller, Yoshua Bengio, Yann Dauphin, and Xavier Glorot. Higher order contractive auto-encoder. In *Machine Learning and Knowledge Discovery in Databases*, pages 645–660. Springer, 2011a.

378 Salah Rifai, Pascal Vincent, Xavier Muller, Xavier Glorot, and Yoshua Bengio. Contractive auto-  
379 encoders: Explicit invariance during feature extraction. In *Proceedings of the 28th International*  
380 *Conference on Machine Learning (ICML-11)*, pages 833–840, 2011b.

381 M. Salzmann, R. Urtasun, and P. Fua. Local deformation models for monocular 3D shape recovery.  
382 In *IEEE Conference on Computer Vision and Pattern Recognition*, CVPR, pages 1–8, 2008.

383 Ercan Solak, Roderick Murray-Smith, E. Solak, William Leithead, Carl Rasmussen, and Douglas  
384 Leith. Derivative observations in gaussian process models of dynamic systems, 2003.

385  
386  
387  
388  
389  
390  
391  
392  
393  
394  
395  
396  
397  
398  
399  
400  
401  
402  
403  
404  
405  
406  
407  
408  
409  
410  
411  
412  
413  
414  
415  
416  
417  
418  
419  
420  
421  
422  
423  
424  
425  
426  
427  
428  
429  
430  
431